

Supporting information

Secondary Lateral Growth of MAPbI₃ Grains for Efficient Perovskite Solar Cells

Chengbo Li^{a,b}, Aili Wang^{a,b}, Lisha Xie^{a,b}, Xiaoyu Deng^{a,b}, Kejun Liao^{a,b}, Jin-an Yang^{a,b}, Yong
Xiang^a, Feng Hao^{a,b,*}

^a School of Materials and Energy, University of Electronic Science and Technology of China,
Chengdu, 610054, China

^b Center for Applied Chemistry, University of Electronic Science and Technology of China,
Chengdu 611731, China

* E-mail: haofeng@uestc.edu.cn

Experimental Section

Materials: Nickel acetate tetrahydrate (Adamas-beta, 98%), ethanol (General-Reagent, 99.7%), isopropanol (General-Reagent, 99.7%), chlorobenzene (CB, Sigma-Aldrich, 99.8%), anhydrous dimethyl sulfoxide (DMSO, Sigma-Aldrich, 99.9%), anhydrous N,N-dimethylformamide (DMF, Sigma-Aldrich, 99.8%), Methylammonium iodide (MAI, Great-Cell, 99.9%), lead(II) iodide (PbI₂, Aladdin, 99.9%), silver (Trillion Metals, 99.9%), PC₆₁BM (Luminescence Technology, 99.5%), were received and used without any further purification.

Perovskite Precursor: The perovskite precursor solution was prepared from a mixture of MAI (0.5M) and PbI₂ (0.5M) in DMF: DMSO 3: 1 (v/v). Then, the mixed solution was magnetically stirred for about 1 h at room temperature until the turbid solution turns into a clear yellow solution.

Perovskite Fabrication: Perovskite solar cells were fabricated on fluorine-doped tin oxide (FTO) conducting glass. FTO was cleaned using detergent, deionized water, ethanol, acetone, and isopropanol for 20 min, respectively. Then, the substrates were treated under UV ozone for another 15 min after nitrogen stream drying. Using a mixture of ethylene glycol and ethylenediamine as a solvent, spin-coating 0.4 M nickel acetate tetrahydrate for 30 s on a substrate heating to 120 °C to deposit a 15 nm thick NiO_x hole transport layer. The compact NiO_x layer was then annealed at 350 °C for 1 hour in an oven. The perovskite layer was spin-cast on the heated (150 °C) FTO/NiO_x substrates from the warm (70 °C) perovskite precursor solution at a speed of 4000 rpm for 30 s, after the spin coating process, the substrate was quickly transferred from the airbox to the glove box, the substrate was annealed at 90 °C for 2 min on the hotplate. Hot-casting preparation method has other applications in our group. Then 50 µl of a mixed solvent of EtOH/CB was dropped into the substrate at a speed of 7000 rpm for 30 s. Then down to room temperature, an electron-transporting layer was coated with a solution of PC₆₁BM dissolved in chlorobenzene (20 mg mL⁻¹) at a speed of 4000 rpm for 30 s and then followed by transferring the thin films onto the hotplate at 60 °C for 1 min. a saturated PEI solution in isopropanol (1mg mL⁻¹) was spin-coated at a speed of 4000 rpm for 30 s. Finally, a 100 nm thick silver electrode was deposited by thermal evaporation under high vacuum conditions.

Characterization

The crystalline phase and purity of the as-obtained films were studied using a MiniFlex 600 (Rigaku) X-ray diffractometer with Cu K α radiation ($\lambda = 0.15406$ nm, 40 kV, 15 mA). The UV-vis spectra of the perovskite films were measured using a UV-2600 spectroscope (Shimadzu) with an integration sphere. Steady-state PL spectroscopy and TRPL decay measurements were performed using a FluoTime 300 (PicoQuant). The J - V characteristics of the solar cell devices were measured using a Keithley 2400 source meter and a solar simulator (San-EI Electric) with standard AM1.5G (100 mW cm $^{-2}$) illumination under ambient conditions. The light intensity of the solar simulator was calibrated with an AK-200 standard silicon solar cell (Konica Minolta). J - V curves for all devices were obtained by masking the cells with a metal mask with an area of 0.096 cm 2 . Monochromatic IPCE spectra were measured using an QE-R (Enlitech). EIS, SCLC, and MOTS measurements were carried out on a CHI 660E electrochemical workstation (CH Instruments Inc.). Photo-CELIV current transients were carried out on a Paios (Fluxim).

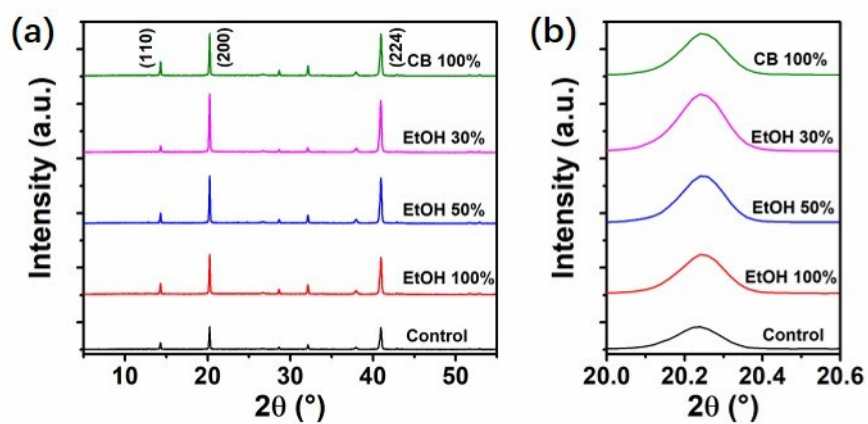


Figure S1. (a) XRD pattern of MAPbI₃ perovskite films deposited on FTO substrate post-treated with different concentration of EtOH; and (b) magnified XRD pattern at (200) lattice plane for MAPbI₃ perovskite films.

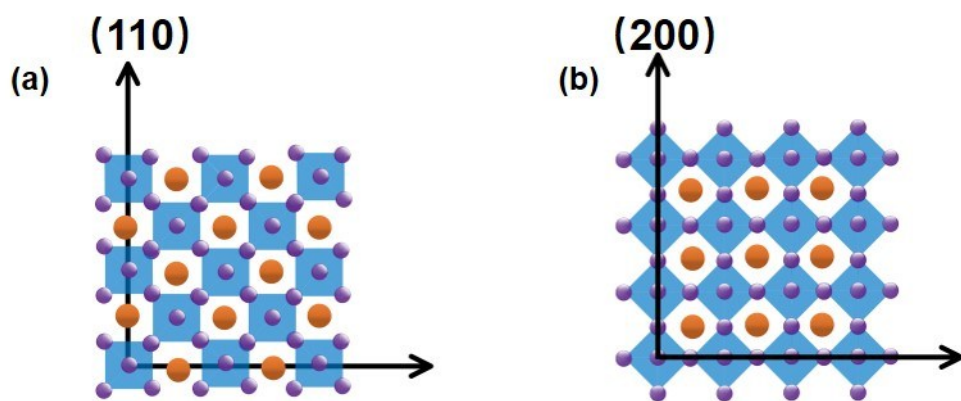


Figure S2. The schematic diagram of (a) the crystals employed $(h\ k\ 0)$ ($h = k$) orientation and (b) $(h\ 0\ 0)$ orientation.

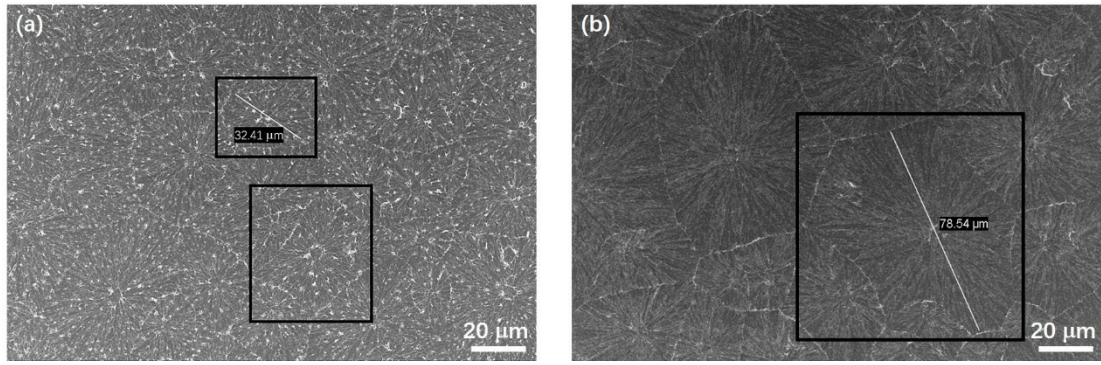


Figure S3. SEM images of (a) MAPbI₃, (b) 30% EtOH post-treated film.

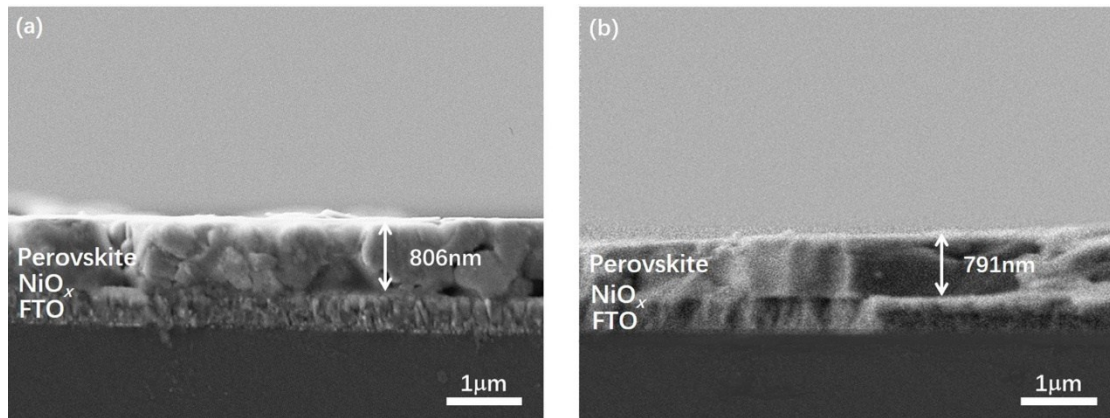


Figure S4. Cross-sectional SEM images of (a) MAPbI₃, (b) 30% EtOH post-treated film.

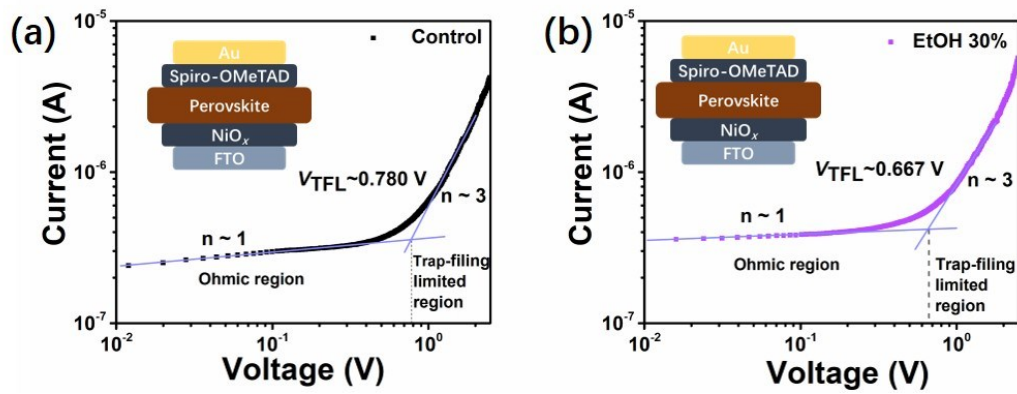


Figure S5. Dark current - voltage curve of (a) pristine and (b) 30% EtOH post-treated devices with a structure of FTO/NiO_x/perovskite/Spiro-OMeTAD/Au.

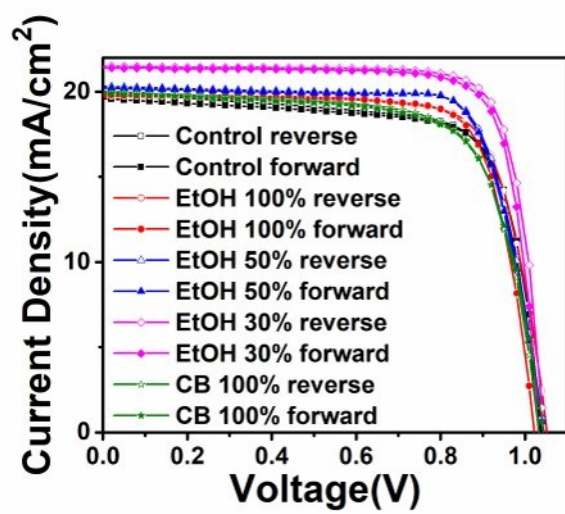


Figure S6. Photovoltaic performance of the devices with and without EtOH post treatment.

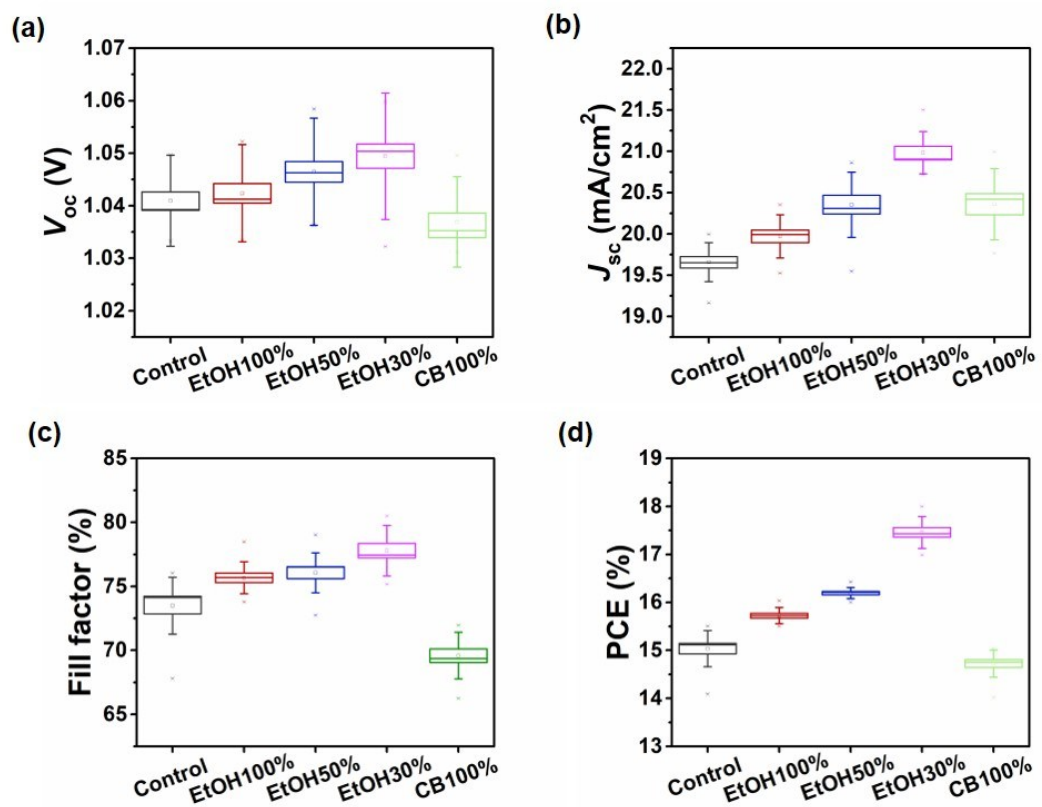


Figure S7. (a–d) Statistical distribution of the photovoltaic parameters for MAPbI₃ perovskite films post-treated with different concentration of EtOH. (a) distribution of V_{oc} ; (b) distribution of J_{sc} ; (c) distribution of FF; (d) distribution of PCE.

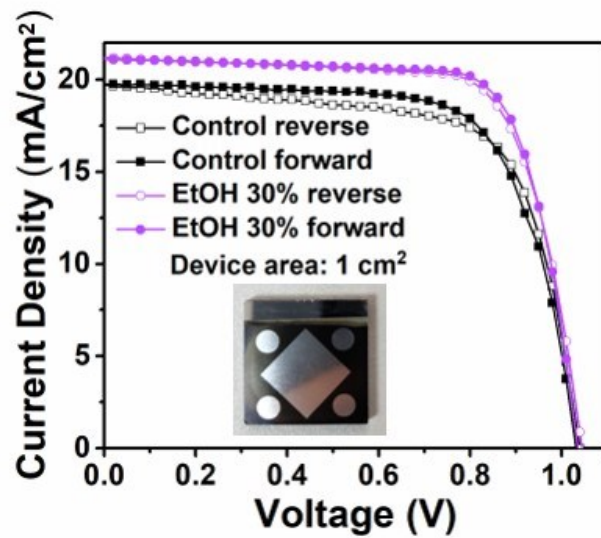


Figure S8. Photovoltaic performance of the large-area devices (1 cm²) with and without EtOH post treatment. The inset shows the photograph of as-fabricated large-area device in the center together with four regular size device in this work.

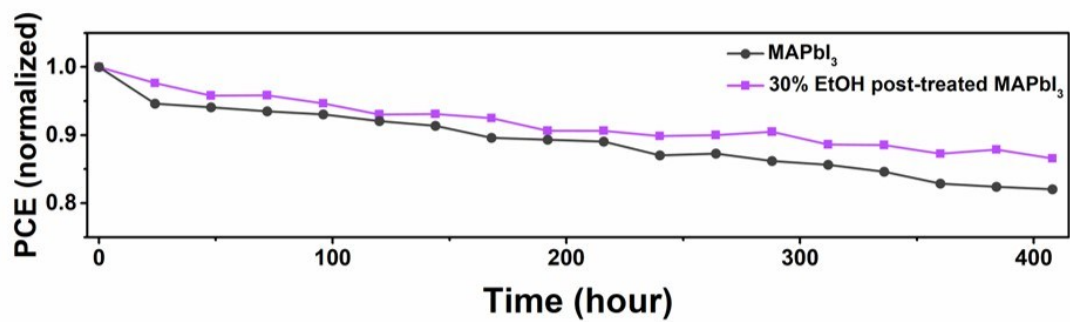


Figure S9. Normalized PCE curves for MAPbI₃ (black) and 30% EtOH post-treated MAPbI₃ (purple) perovskite solar cells without encapsulation and stored in a nitrogen glovebox.

Table S1. Summary of devices' electron lifetimes with and without (w/o) EtOH post treatment.

Structure	A_1	τ_1 (ns)	A_2	τ_2 (ns)	τ_{av} (ns)
Perovskite	0.65	19.58	0.50	40.14	32.80
Perovskite/EtOH	0.30	17.12	0.65	80.29	57.32

Table S2. Slope of the Mott - Schottky plots and doping densities of ETLs.

\square	Slope	N_d (cm ⁻³)	V_{bi} (V)
Control	-7.68×10^{17}	2.85×10^{14}	0.284
EtOH 30%	-3.83×10^{17}	5.71×10^{14}	0.309

Table S3. Electron trap density (n_e) of MAPbI₃ with and w/o 30% EtOH post treatment.

	Control	EtOH 30%
n_t (cm ⁻³)	1.17×10^{16}	8.63×10^{15}

Table S4. Photovoltaic parameters of the devices with and w/o EtOH post treatment.

\square	J_{sc} (mA/cm ²)	V_{oc} (V)	Fill Factor (%)	Efficiency (%)
Control Reverse	19.92	1.04	73.41	15.15
Forward	19.60	1.04	74.50	15.12
Average	19.62±0.18	1.04±0.01	73.5±2.13	15.04±0.36
ETOH-100% Reverse	19.72	1.05	75.87	15.74
Forward	19.80	1.02	76.66	15.51
Average	19.97±0.25	1.04±0.01	75.67±1.2	15.72±0.16
ETOH-50% Reverse	20.31	1.04	76.55	16.24
Forward	20.22	1.04	76.61	16.16
Average	20.35±0.38	1.05±0.01	76.06±1.49	16.19±0.11
ETOH-30% Reverse	21.50	1.04	80.52	18.00
Forward	21.40	1.03	79.98	17.65
Average	21.01±0.31	1.05±0.01	78.80±1.04	17.04±0.47
CB-100% Reverse	20.50	1.03	70.67	14.98
Forward	20.39	1.04	69.25	14.82
Average	20.33±0.41	1.04±0.01	69.59±1.75	14.73±0.27

Table S5. The charge carrier mobility of MAPbI₃ with and w/o 30% EtOH post treatment.

	A (V/s)	t_{\max} (μ s)	j_0 (mA/cm ²)	Δj (mA/cm ²)	μ (cm ² /Vs)
Control	40000	2.88	0.793	0.744	1.84×10^{-3}
EtOH 30%	40000	2.64	0.563	0.482	2.23×10^{-3}